An Acad Bras Cienc (2025) 97(Suppl. 3): e20250559 DOI 10.1590/0001-3765202520250559
Anais da Academia Brasileira de Ciências | *Annals of the Brazilian Academy of Sciences*
Printed ISSN 0001-3765 I Online ISSN 1678-2690
www.scielo.br/aabc | www.fb.com/aabcjournal

ENGINEERING SCIENCES

Biodegradable nanocomposite films containing combined ZnO and TiO_2 nanoparticles in PBAT: A strategy to mitigate microplastic persistence from food packaging

CAMILA S.G. FERREIRA, PRISCILA S. E SOUZA, DILMA S. LACERDA, FERNANDO A.M. RODRIGUES & GISELE CRISTINA V. IULIANELLI

Abstract: The persistent accumulation of microplastics from synthetic polymers threatens ecosystems and biodiversity. The use of biodegradable and compostable materials as alternatives to conventional plastics in food packaging has shown promise, particularly with the development of nanocomposites that can be tailored to meet market demands. In this study, ZnO and TiO_2 nanoparticles were combined and incorporated into a biodegradable poly(butylene adipate-co-terephthalate) (PBAT) matrix at varying concentrations, forming a novel ternary PBAT/ZnO/TiO_2 system. The films produced via melt processing were characterized using conventional and non-conventional techniques to evaluate their thermal, morphological, chemical, wettability, and biosafety properties. The results indicated that the combined addition of ZnO and TiO_2 slightly reduced the thermal stability and crystallinity of PBAT, while increasing surface hydrophilicity. These features may contribute to accelerated degradation and reduced environmental persistence. Furthermore, improvements in the elastic modulus and enhanced biosafety were observed across all tested concentrations. These findings suggest that the prepared nanocomposites, particularly at 0.75 and 1 wt%, not only possess properties suitable for food packaging applications but also demonstrate potential to mitigate environmental persistence through accelerated degradation. Therefore, this study supports the development of environmentally friendly materials for food packaging, addressing the urgent need to reduce microplastic pollution.

Key words: PBAT, ZnO, TiO_2, biodegradable nanocomposites, food packaging, microplastics.

INTRODUCTION

The fragmentation of larger plastics into microparticles represents a silent and growing threat to ecosystems. Microplastics, defined as particles smaller than 5 mm, are currently among the most pressing environmental crises. Their diminutive size amplifies their potential for contamination, earning them significant attention in ecotoxicity studies and for their biomagnification effects within the food chain (Yadav et al. 2024).

When ingested by marine organisms, microplastics infiltrate the food chain, contaminating fish and other organisms that are part of the human diet. Additionally, these plastic fragments exhibit a high capacity to bind with toxic substances in the environment, exacerbating their harmful effects. In soil, microplastics degrade its quality, negatively impact plant health, and disrupt microbial life. When inhaled or ingested, these particles can cause human health issues such as inflammation and respiratory problems (Le et al. 2024).

The growing proliferation of microplastic particles across diverse environments presents an urgent environmental challenge. To address this issue, the development of biodegradable and compostable materials incorporating nanoparticles has emerged as a promising solution to mitigate their impact.

Biodegradable polymer-based nanocomposites for food packaging present opportunities to not only enhance the properties and efficiency of these materials but also contribute to reducing food waste by extending the shelf life of fresh products. Additionally, these materials reduce the volume of non-biodegradable packaging waste in landfills. Recent advances in food packaging materials have closely followed developments in nanotechnology (Mendes et al. 2019).

Among biodegradable polymers, poly(butylene adipate-co-terephthalate) (PBAT) is considered safe and has been approved by the Food and Drug Administration (FDA) for food packaging applications due to its non-toxicity and absence of heavy metals (Muroi et al. 2017). It also meets several international biodegradability and compostability certifications, including the European Standard DIN EN 13432, the North American ASTM D-6400, and the Japanese GreenPLA Standard (Muroi et al. 2017, Zehetmeyer et al. 2016).

PBAT is a biodegradable copolyester with an accelerated degradation process facilitated by environmental enzymes, ultimately generating water, carbon dioxide, and biomass (La Fuente et al. 2023). It is synthesized through the reaction of 1,4-butanediol, adipic acid, and terephthalic acid (La Fuente et al. 2023). In terms of composition, 43% of PBAT's structure is attributed to the butylene terephthalate (BT) group, which contributes to its mechanical and thermal properties, while the remaining 57% corresponds to the butylene adipate (BA) group, which imparts flexibility and biodegradability (Tavares et al. 2018). Another key feature of PBAT is its similarity to low-density polyethylene (LDPE), making it a potential substitute for conventional polymers widely used in industry and associated with high environmental impacts (Jian et al. 2020, Rameshkumar et al. 2020).

Zinc oxide (ZnO) is one of the most widely used metal oxides due to its notable antimicrobial properties. It is recognized as Generally Recognized as Safe (GRAS) by the U.S. Food and Drug Administration (FDA) and is also an essential micronutrient for humans (Batool et al. 2022, Cunha et al. 2022, Rizky Salsabila et al. 2023, Da Rocha et al. 2023). ZnO has gained attention for its chemical, optical, mechanical, electrical, and magnetic properties (Ahmad et al. 2022, Hong et al. 2006, Mayrinck et al. 2014, Rizky Salsabila et al. 2023, Smaoui et al. 2023). Its morphology and size, determined by its microstructure, directly influence these properties (Mayrinck et al. 2014).

The use of TiO_2 nanoparticles (TiO_2 NPs) in food packaging offers high photocatalytic activity, good biocompatibility, non-toxicity, and potent antibacterial functionality due to their high specific surface area (Chen et al. 2020, Zhang & Rhim 2022). TiO_2 nanoparticles can enhance the antimicrobial properties of active films and act as crosslinking agents, improving the mechanical and barrier properties of films. Their addition can also provide ethylene-scavenging activity, which is critical for extending the shelf life of products (Charoensri et al. 2021, Hou et al. 2019, Kodithuwakku et al. 2022, Mesgari et al. 2021, Wang et al. 2014, Yang et al. 2014).

In this study, varying concentrations of ZnO and TiO_2 nanoparticles were combined and incorporated into the PBAT matrix using melt processing. This method was selected for its economic advantages, high industrial productivity, and absence of residues. The goal is to develop biodegradable nanocomposite films, aiming to reduce the environmental impacts of conventional non-biodegradable packaging while improving the properties of PBAT for such applications.

The properties of the novel systems developed in this study (PBAT/ZnO/TiO_2) were systematically evaluated through FTIR (Fourier Transform Infrared Spectroscopy), FEG-SEM (Field Emission Scanning Electron Microscopy), XRD (X-ray Diffraction), TGA (Thermogravimetric Analysis), tensile mechanical testing, contact angle measurement (Wettability), and a non-conventional water activity analysis for food packaging. The goal was to identify potential improvements in PBAT properties and determine the most promising systems for food packaging applications aimed at mitigating microplastic persistence in the environment.

MATERIALS AND METHODS

Materials

The polymeric matrix used in this study was poly(butylene adipate-co-terephthalate) (PBAT), commercially known as Ecoflex® F Blend C 1200, supplied by BASF S.E. (Florham Park, NJ, USA). This material has a density between 1.25 and 1.27 g/cm³ (at 23°C), an intermediate melt flow index (2.5–4.5 g/10 min, 190°C and 2.16 kg), and a melting point range of 110–120°C. The polymer is white and supplied as spherical pellets approximately 5 mm in size. Zinc oxide nanoparticles (ZnO NPs) were obtained from Sigma-Aldrich ReagentPlus® (particle size < 100 nm, purity ≥ 99.5%), with a specific surface area of 10–25 m²/g. These particles are odorless, fine, and white in appearance. Titanium dioxide nanoparticles (TiO_2 NPs), anatase phase, were also supplied by Sigma-Aldrich ReagentPlus® (particle size < 25 nm, purity ≥ 99.7%), with a specific surface area of 45–55 m²/g. Like ZnO NPs, these particles are odorless, fine, and white.

Preparation of nanocomposites

All nanocomposite films were prepared using a single-screw mini-extruder (model 1626, Ax Plásticos), equipped with a film roller system operating at 50 rpm. The extrusion speed was set at 60 rpm, and the temperature profile across the three heating zones was maintained at 130°C/130°C/135°C, respectively.

Prior to extrusion, PBAT pellets were ground and mixed with ZnO and TiO_2 nanoparticles at varying concentrations, maintaining a 1:1 ratio of both nanoparticles. The nanoparticle concentrations tested were 0.25, 0.50, 0.75, 1.00, 1.50, and 2.50 wt%. The mixtures were homogenized in a solid mixer for 30 minutes to ensure uniform distribution.

Characterization of the produced films

Fourier Transform Infrared Spectroscopy (FTIR)

FTIR analysis was performed using a PerkinElmer Frontier FT-IR/FIR spectrophotometer (Spectrum, version 10.4.2, serial number 98737), equipped with a Platinum ATR accessory. Spectra were acquired in the spectral range of 4000 to 400 cm^{-1}, with a resolution of 4 cm^{-1} and 60 scans per sample.

Thermogravimetric Analysis (TGA)

Thermogravimetric analysis was conducted using a TA Instruments Q500 Thermogravimetric Analyzer, with a temperature precision of ±2 °C. Samples were heated from 25 °C to 700 °C at a rate of 10 °C/min under a nitrogen atmosphere with a constant flow rate of 60 mL/min.

X-Ray Diffraction (XRD)

The crystalline structure of PBAT and its nanocomposite films was evaluated using X-ray diffraction (XRD). Diffractograms were obtained using a Rigaku Ultima IV diffractometer equipped with a copper monochromator (CuKα, λ = 1.54 Å) and a scintillation counter detector. Analyses were performed at room temperature under operational conditions of 40 kV and 20 mA, with a scanning speed of 0.05°/s over a 2θ range of 2°–60°. The degree of crystallinity (Xc) was calculated using Origin® software, according to the equation $Xc (\%) = I_C / (I_C + I_A) \times 100$, where: I_C is the integrated area under the crystalline peaks and I_A is the area of the amorphous halo. Peak deconvolution was performed using a Gaussian function (Iulianelli et al. 2023).

Field Emission Scanning Electron Microscopy (FEG-SEM)

The morphological analysis of nanocomposite films was performed using a TESCAN MIRA FEG-SEM (4th generation), equipped with a Schottky FEG, low-vacuum mode (1–700 Pa), and LMU detector. Sample surfaces were coated with a thin gold layer (using a BAL-TEC SCD005 sputter coater) at a current of 30 mA for 150 seconds to ensure conductivity. Nanocomposite films were cryosectioned in liquid nitrogen prior to coating to allow visualization of nanoparticle dispersion within the PBAT matrix. Micrographs were acquired at magnifications of up to 10,000×, with an accelerating voltage of 10 keV.

Tensile Mechanical Testing

Tensile testing was conducted using an Instron Universal Testing Machine (model 4204) in accordance with ASTM D882-18 standards. For each film group, specimens (250 mm length × 25 mm width) were conditioned for 48 hours at 23 ± 2 °C and 50 ± 5% relative humidity. Specimen fabrication involved: (1) hot pressing at 160 °C under 10 tons pressure for 180 s with five degassing cycles, followed by (2) pressure-maintained cooling (10 tons, 130 s) in a water-circulated hydraulic press. Tests were performed using a 1 kN load cell at a crosshead speed of 10 mm/min. At least five valid replicates were collected for each group of samples to calculate the mean value and standard deviation.

Contact Angle Measurements (Surface Wettability)

Contact angle measurements were performed using an OCA-15EC (Dataphysics Instruments). A 1 µL droplet of water was placed on the film surface using a precision syringe. Contact angles on both sides of the droplet (left and right) were measured, and the reported value corresponds to the average of five measurements, conducted under consistent lighting and at 20 °C. Contact angle values were classified as follows: hydrophilic (0°–<90°), hydrophobic (90°–150°), and superhydrophobic (>150°) (Yin et al. 2010).

Water Activity (aW)

The water activity (aW) of the samples was measured using an AquaLab 4TE (Meter Group Latam Ltda) with a dewpoint system, offering an accuracy of ±0.0030 aW. The materials were analyzed as received, without any additional preparation. All samples were stored at room temperature in sealed containers, protected from humidity, light, and heat. Measurements were performed in triplicate to ensure reliability. The threshold water activity levels for microbial growth are 0.90 aW for most pathogenic bacteria, 0.70 aW for spoilage molds, and 0.60 aW as the lower limit for all microorganisms (Beuchat 1982).

RESULTS AND DISCUSSION

Fourier Transform Infrared Spectroscopy (FTIR)

The ZnO spectrum (Figure 1a) exhibited absorption bands between 561 and 997 cm⁻¹, attributed to Zn-O bond deformation and stretching. A broad band at 3423 cm⁻¹ represents the stretching vibrations of O-H bonds, possibly indicating moisture. Similar FTIR results for ZnO NPs have been reported in the literature (De Peres et al. 2019, Handore et al. 2014, Janaki et al. 2015, Masud et al. 2020, Quadri et al. 2017, Valerio et al. 2019).

For TiO_2 NPs (Figure 1b), characteristic absorption bands were observed, including a band at 3368 cm^{-1} corresponding to water molecule stretching associated with TiO_2 and a small band at 1640 cm^{-1} related to the angular deformation and stretching vibrations of hydroxyl groups on the nanoparticle surface. The band at 644 cm^{-1} corresponds to Ti-O vibrations, as documented in previous studies (Al-amin et al. 2016, Chougala et al. 2017, Praveen et al. 2014, Rajakumar et al. 2012, Valentim et al. 2014, Venkatesan & Rajeswari, 2017b).

The FTIR spectrum of pure PBAT (Figure 1c) displayed a sharp band at 727 cm^{-1}, associated with the vibrations of methylene ($-CH_2-$) groups in the polymer structure. A band at 1268 cm^{-1}

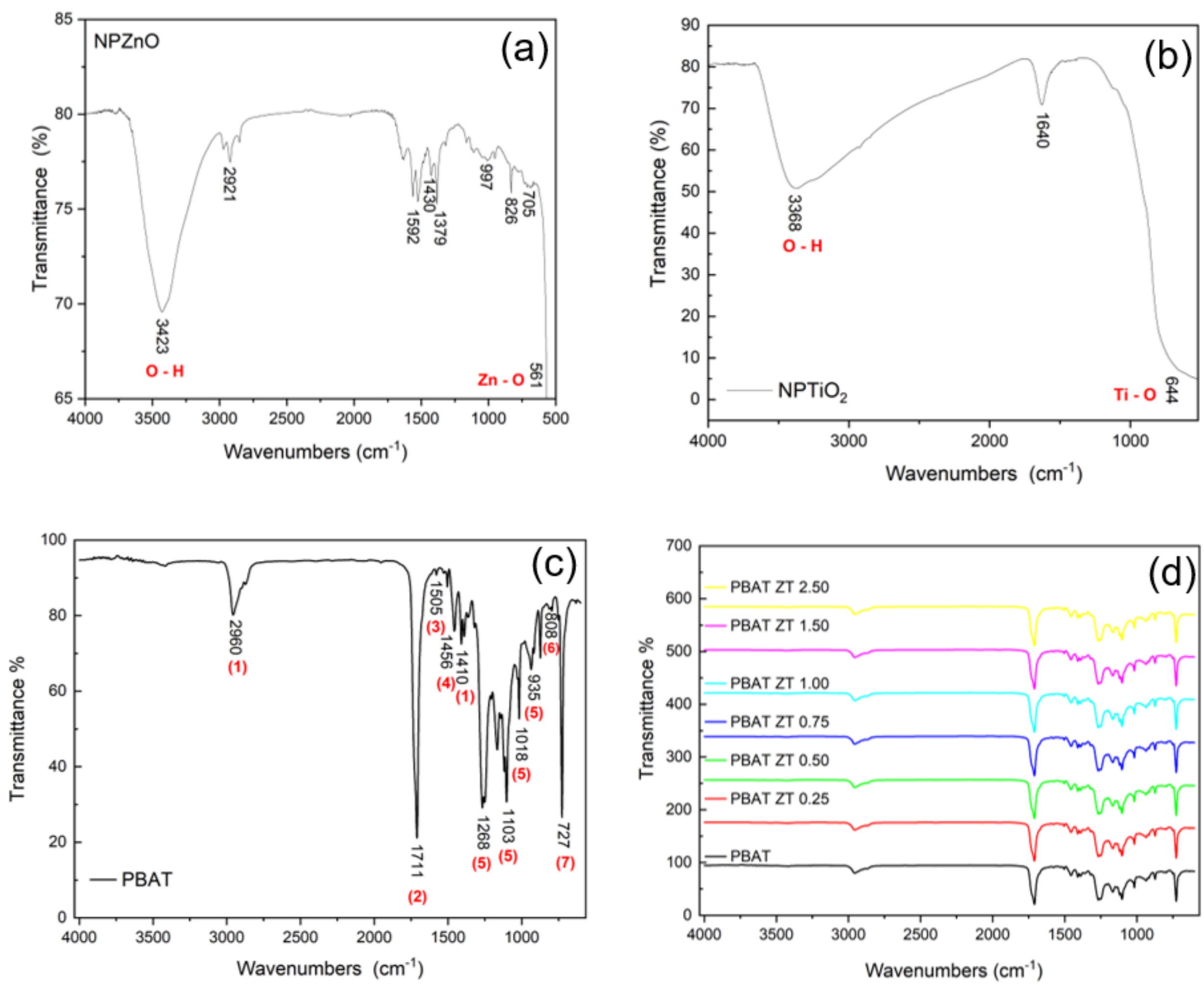

Figure 1. FTIR spectra of: (a) ZnO, (b) TiO_2, (c) pure PBAT, and (d) PBAT/ZnO/TiO_2 nanocomposites.

corresponds to the stretching of C-O bonds in ester groups, while the most intense absorption band, observed at 1711 cm^{-1}, is attributed to the carbonyl group (C=O) of the ester linkage. The band around 3000 cm^{-1} indicates C-H stretching in aliphatic and aromatic portions, and the bands between 1018 and 808 cm^{-1} are related to substituted benzene rings (Cardoso et al. 2019, Da Silva et al. 2020).

The combined inclusion of ZnO and TiO_2 NPs (Figure 1d) did not significantly alter the main vibrational bands in the FTIR spectrum of PBAT nanocomposites compared to pure PBAT (Figure 1c). The characteristic peaks of pure PBAT remained predominant, with no notable peaks corresponding to ZnO or TiO_2, likely due to the low nanoparticle concentrations incorporated.

Thermogravimetric Analysis (TGA)

The thermogravimetric data for pure PBAT, ZnO, TiO_2, and PBAT/ZnO/TiO_2 nanocomposites are summarized in Table I and TG and DTG curves are presented in Figure 2 .

As shown in Figure 2 (b), the addition of combined ZnO and TiO_2 nanoparticles increased the number of degradation stages with rising nanoparticle concentrations. Composites containing 0.25–0.50 wt.% exhibited a single degradation stage, whereas formulations with 0.75–2.50 wt.% displayed three distinct stages. A progressive decrease in T_{Onset} and T_{Max} values was observed as nanoparticle concentration increased. These results can be attributed to photocatalytic and thermocatalytic properties of ZnO and TiO_2 nanoparticles, which can accelerate polymer degradation by facilitating the breaking of molecular bonds under heat exposure. The most significant reduction was observed in the formulation containing 2.5 wt.% ZnO/TiO_2, with approximately a 40°C decrease in T_{Onset}. This reduction could be due to nanoparticle agglomeration, which is more pronounced at higher concentrations, leading to localized hotspots that lower the degradation temperature. This decrease in the thermal stability does not hinder the application of these materials for food packaging. Moreover, the accelerated degradation after disposal could offer environmental benefits. The increased catalytic activity of ZnO and TiO_2 nanoparticles may help reduce the persistence of microplastics in the environment.

Table I. Quantitative data obtained from TGA for nanoparticles and PBAT/ZnO/TiO_2 systems.

Samples	T_{Onset} (°C)	T_{Max} (°C)
NPZnO	N.D.	N.D.
NPTiO_2	N.D.	N.D.
PBAT	381	406
PBAT ZT 0.25	376	404
PBAT ZT 0.50	362	397
PBAT ZT 0.75	353	375
PBAT ZT 1.00	356	371
PBAT ZT 1.50	323	353
PBAT ZT 2.50	340	368

N.D. Not Detected.

X-ray Diffraction (XRD)

Pure PBAT exhibited a semicrystalline profile with diffraction peaks at 2θ = 16.05°, 17.5°, 21.15°, 23.15°, and 24.8°, corresponding to the (011), (010), (101), (100), and (111) crystalline planes, respectively (Bheemaneni et al. 2018, Castro et al. 2020, Da Silva et al. 2020). This pattern is typical for PBAT, a biodegradable polymer that displays both crystalline and amorphous regions. The degree of crystallinity (Xc) was 27%, consistent with literature values and manufacturer specifications (Castro et al. 2020, Da Rocha et al. 2023).

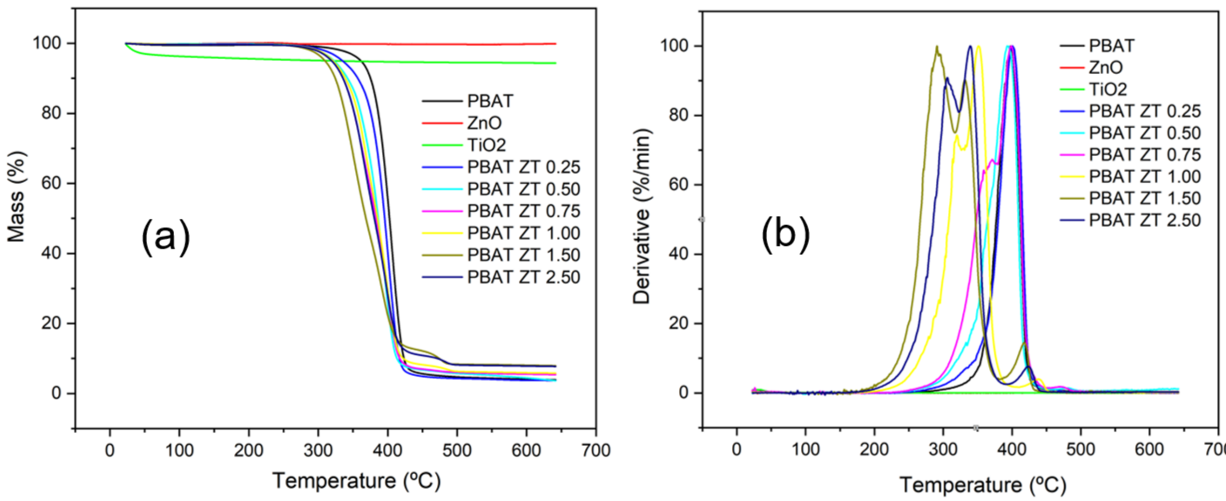

Figure 2. TG curves (a) and DTG curves (b) obtained for pure PBAT, ZnO, TiO_2, and PBAT/ZnO/TiO_2 nanocomposites.

For ZnO, characteristic peaks at 2θ = 32.2°, 33.9°, 36.2°, 47.3°, and 56.4° were observed, corresponding to (100), (002), (101), (102), and (110) planes, respectively (Pascariu et al. 2020, Thiyagu et al. 2022). The crystalline peaks of ZnO observed in the XRD patterns confirm ZnO nanoparticles with the characteristic wurtzite structure, known for its stability and activity in catalytic reactions. TiO_2 displayed a prominent peak at 2θ = 24.8° (101). The crystalline phase of TiO_2 observed in the XRD analysis suggests the presence of anatase, which is commonly employed in photocatalytic applications due to its high surface area and reactivity under light exposure (Arssanasuwan et al. 2020, Venkatesan & Rajeswari 2017b).

As shown in Figure 3, formulations containing 0.25–0.75 wt.% of combined nanoparticles exhibited only the characteristic crystalline peaks of pure PBAT. This suggests that, at low nanoparticle concentrations, the nanoparticles are well-dispersed within the polymer matrix, without significantly altering the crystalline structure of the PBAT. However, as the nanoparticle concentration increased beyond 1 wt.%, new peaks corresponding to the ZnO and TiO_2 nanoparticles became evident. This indicates that, at these concentrations, the nanoparticles begin to form crystalline structures that are detectable by XRD, suggesting that the nanoparticles are no longer fully dispersed and may be agglomerating. Furthermore, the addition of ZnO and TiO_2 nanoparticles caused a reduction in the intensity of PBAT diffraction peaks for systems containing 1.5 and 2.5 wt.% of combined nanoparticles, indicating that the addition of nanoparticles affects the crystalline structure of PBAT.

Compared to pure PBAT (Xc = 27%), the nanocomposite films containing ZnO and TiO_2 nanoparticles exhibited a slight reduction in the degree of crystallinity (Xc ≈ 22%), independent of nanoparticles concentration (0.25–2.50 wt.%). XRD analysis confirmed that the combined addition of ZnO and TiO_2 influenced the microstructural organization, resulting in a modest decrease in crystallinity. This correlates with enhanced biodegradability, as amorphous regions are more susceptible to hydrolytic/enzymatic attack, a key advantage for environmental sustainability. Thus, the presence of ZnO and TiO_2 nanoparticles could lead to a synergistic effect, where both the nanoparticles'

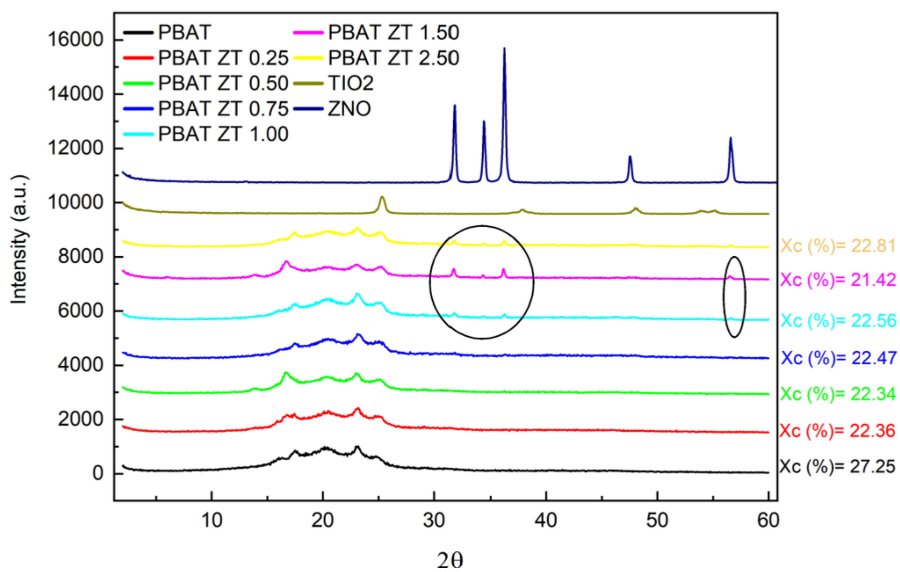

Figure 3. XRD diffractograms and crystallinity degree obtained for pure PBAT, ZnO, TiO_2, and PBAT/ZnO/TiO_2 nanocomposites.

catalytic properties and the reduced crystallinity contribute to accelerated material degradation.

Field Emission Scanning Electron Microscopy (FEG-SEM)

The FEG-SEM images for the ZnO and TiO_2 samples are shown in Figure 4 (a) and (b), respectively. For NPZnO (Figure 4 (a)), the analysis of the image reveals a wide variety of morphologies, including spherical, irregular hexagonal, cylindrical structures, nanocrystal agglomerates, and cubic ZnO crystals, among others. Several authors have reported similar morphological variations for NPZnO in previous studies (Batool et al. 2022, De Souza et al. 2022, Pascariu et al. 2020, Thabit & Kabir 2018, Venkatesan &Rajeswari 2017a).

Figure 4 (b) shows the FEG-SEM image obtained for $NPTiO_2$. The image reveals large agglomerates of $NPTiO_2$ with distinct sizes, ranging from approximately 27 to 36 nm, and a morphology corresponding to a roughly spherical shape. Similar morphological results have been reported in the literature (Haider et al. 2017, Jaybhaye et al. 2022, Pavani et al. 2023, Sang et al. 2014, Suwarnkar et al. 2014).

The pure PBAT film (Figure 5 a-) exhibited a dense, homogeneous structure with a few distributed pores, without imperfections, cracks, or holes, as observed by other authors (Arssanasuwan et al. 2020, Capelezzo et al. 2018, Da Rocha et al. 2023).

As observed, the photomicrographs shown in Figure 5 (b-f) illustrate the dispersion of ZnO and TiO_2 nanoparticles combined in the PBAT polymer matrix. It was found that formulations with higher concentrations (1.50 wt.% and 2.50 wt .%) exhibited the formation of agglomerates. For lower concentrations, ranging from 0.25 wt.% to 1.00 wt.%, a more homogeneous dispersion and distribution of nanoparticles were observed. This suggests that for the ternary PBAT/ZnO/TiO_2 system, concentrations above 1.5 wt.% are excessive, leading to defects in the PBAT matrix by promoting agglomerate formation.

The broken lines in Figures 5(d) and 5(e) reflect defects created during the cryogenic fracture process performed for the analysis, consistent with observations reported in the literature (Cardoso et al. 2019).

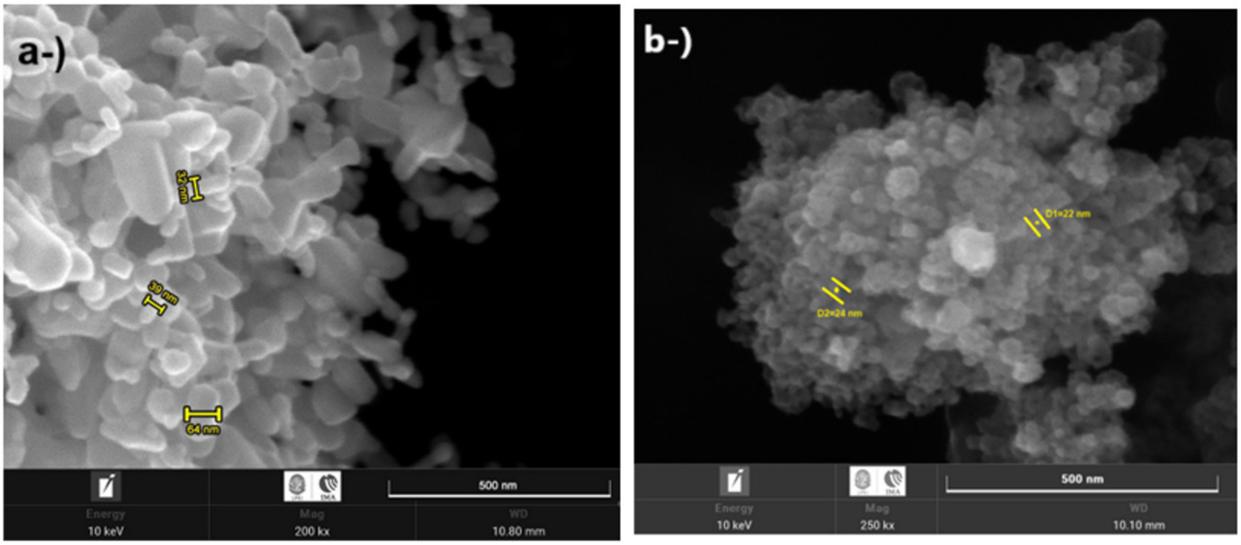

Figure 4. FEG-SEM images of (a-) ZnO nanoparticles and (b-) TiO_2 nanoparticles.

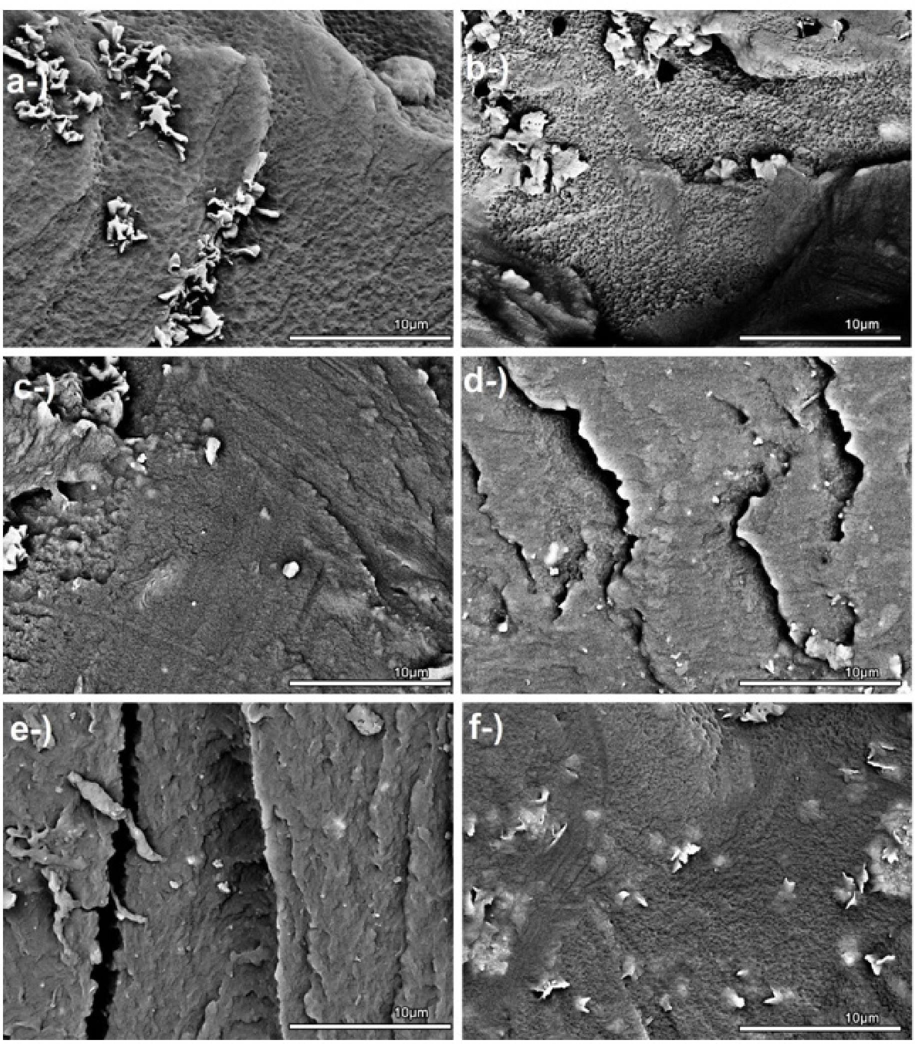

Figure 5. FEG-SEM images of: (a-) Pure PBAT; (b-) PBAT ZT 0.25; (c-) PBAT ZT 0.50; (d-) PBAT ZT 0.75; (e-) PBAT ZT 1.00; (f-) PBAT ZT 1.50 and (g-) PBAT ZT 2.50.

Tensile Mechanical Testing

The results obtained from tensile testing (Figure 6 and Table II) revealed that the Young's modulus (E) of the pure PBAT film was 93.71 MPa, with an elongation at break (ε) of 294.35% and a tensile strength at maximum stress (σ) of 10.96 MPa. These results align with findings reported in the literature (Da Silva et al. 2020). For PBAT nanocomposites, the elastic modulus (E) showed a noticeable increase compared to pure PBAT. The formulation containing 1.5 wt.% nanoparticles exhibited the highest modulus value, reaching 142 MPa, which represents a 53% increase. This enhancement can be attributed to the reinforcing effect of the ZnO and TiO_2 nanoparticles, which, due to their high surface area and strong interaction with the PBAT matrix, restrict the mobility of polymer chains and contribute to the overall rigidity of the nanocomposite films. The nanoparticles may form a network within the polymer, offering

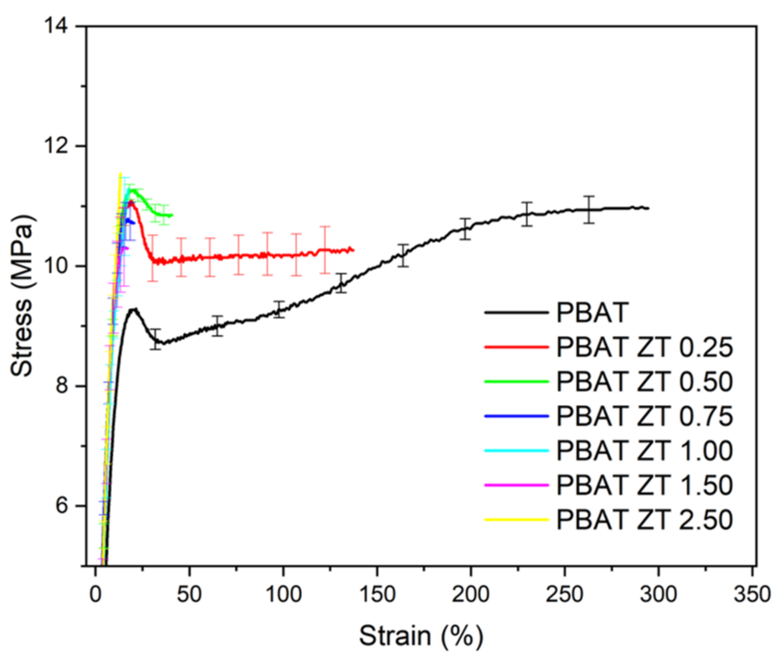

Figure 6. Stress-strain curves of pure PBAT and PBAT/ZnO/TiO_2 nanocomposites.

Table II. Results obtained from the tensile testing for pure PBAT and PBAT/ZnO/TiO_2 systems.

Samples	MaximumTensile Strength (MPa)	Elongation at Break (%)	Young's Modulus (MPa)
PBAT	10.96 ± 0.58	294.35 ± 0.56	93.71± 6.50
PBAT ZT 0.25	11.19 ± 0.32	137.31 ± 0.94	120.65 ± 4.15
PBAT ZT 0.50	11.44 ± 0.43	40.79 ± 0.28	116.29 ± 2.38
PBAT ZT 0.75	11.08 ± 0.80	20.57 ± 0.70	130.44 ± 8.56
PBAT ZT 1.00	10.31 ± 0.53	17.65 ± 0.49	128.48 ± 6.97
PBAT ZT 1.50	10.34 ±1.47	17.14 ± 1.50	142.46 ± 12.70
PBAT ZT 2.50	10.42 ± 1.15	13.17 ± 0.97	125.20 ± 2.46

additional resistance to deformation and thus increasing the modulus. However, at higher concentrations (2.5 wt.%), a slight reduction in the elastic modulus was observed compared to the nanocomposite containing 1.5 wt.% of nanoparticles. This behavior may be associated with the formation of nanoparticle agglomerates, as observed by FEG-SEM, which can create inhomogeneous regions in the matrix, leading to stress concentration points and inefficient load transfer. Similar trends have been reported in other polymer-based nanocomposite systems, where optimal nanoparticle dispersion enhances mechanical properties, while excessive loading leads to particle clustering and structural defects (Sabarish et al. 2024).

Regarding elongation at break (ε), a progressive decrease was observed with increasing nanoparticle concentration. The formulation containing 2.5 wt.% nanoparticles exhibited a significant reduction to 13%, representing a 95% decrease compared to pure PBAT. This reduction can be explained by the introduction of nanoparticles, which may act as physical barriers within the matrix, restricting the mobility of the polymer chains and reducing the material's ability to deform under stress. At higher concentrations, the agglomeration of ZnO and TiO_2 particles could exacerbate this effect, leading to poor interfacial bonding between the nanoparticles and the PBAT matrix, which can further limit the polymer's stretchability.

The tensile strength (σ_max) of the nanocomposites remained statistically unchanged compared to pure PBAT, despite the increase in stiffness. This indicates that while the ZnO and TiO_2 nanoparticles restrict polymer chain mobility, enhancing elastic modulus, their contribution to stress transfer is insufficient to significantly improve σ_max. This behavior can be attributed to the lack of nanoparticle surface functionalization, limiting interfacial adhesion with the PBAT matrix (Pens et al. 2024).

Contact Angle Measurement (Wettability)

The contact angle (θ) of the pure PBAT surface was measured as 83.1°, indicating a slightly hydrophilic surface ($\theta < 90°$). Similar θ values close to 90° for pure PBAT have been reported in the literature (Da Rocha et al. 2023, Da Silva et al. 2020).

As shown in Figure 7, all PBAT/ZnO/TiO_2 nanocomposites exhibited contact angles below 90° (ranging from 59.9° to 71.0°), confirming their hydrophilic nature. A clear trend toward enhanced hydrophilicity was observed with increasing nanoparticle loading (0.25-2.5 wt.%). This enhanced wettability stems from the intrinsic hydrophilic properties of both ZnO and TiO_2 nanoparticles (Ahmad et al. 2022), which dominate the surface characteristics of the nanocomposites. The increased hydrophilicity can facilitate both: (1) hydrolysis, a primary degradation mechanism for biodegradable polymers; and (2) biological degradation via enhanced microbial adhesion and enzymatic activity. This synergistic effect contributes to a reduced environmental persistence, aligning with sustainability objectives for eco-friendly packaging.

Water Activity Analysis

Water activity (aw) is a critical parameter for evaluating the performance of food packaging materials, as it provides essential insights into the availability of free water that can promote microbial growth and trigger undesirable physicochemical reactions. In this study, water activity measurements were conducted to investigate the influence of ZnO and TiO_2 nanoparticles, at different concentrations, on the biosafety of PBAT films. The water activity (aw) values obtained for the PBAT samples, representing the average of five replicates with their respective standard deviations, were as follows: PBAT 0 (control): 0.6 ± 0.0058; PBAT 0.25: 0.58 ± 0.0082; PBAT 0.50: 0.58 ± 0.0082; PBAT 0.75: 0.56 ± 0.0096; PBAT 1.00: 0.56 ± 0.0150; PBAT 1.50: 0.55 ± 0.0050; and PBAT 2.50: 0.55 ± 0.0082. As shown in Figure 8, the incorporation of ZnO and TiO_2 nanoparticles into the PBAT matrix influenced the aw behavior of the films. Notably, all nanocomposites exhibited aw values lower than 0.6, a critical threshold for inhibiting microbial growth. A trend of reduction in aw values was observed with increasing nanoparticle concentrations. This reduction is particularly relevant for food preservation, as aw values below 0.60 are associated with microbiological stability and extended shelf life. Furthermore, lower aw levels can mitigate hydrolytic and oxidative reactions, contributing to the physicochemical stability of packaged food products.

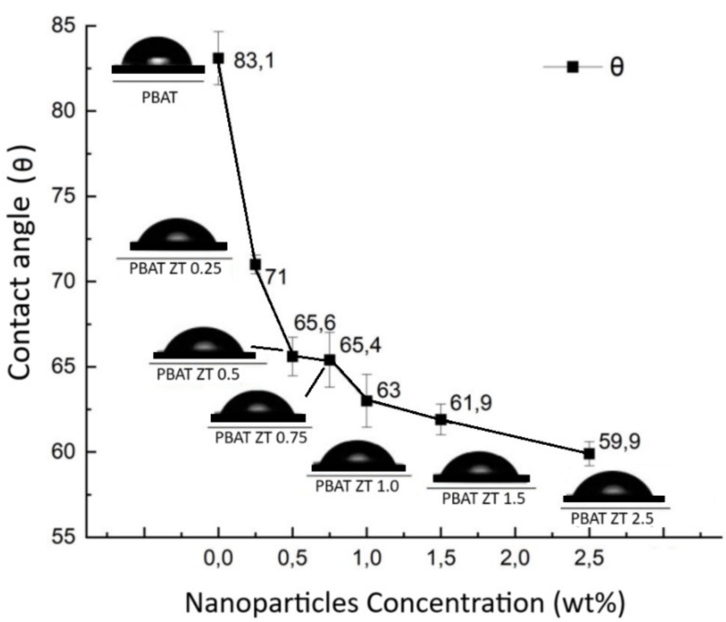

Figure 7. Contact angle measurements of pure PBAT film and PBAT/ZnO/TiO_2 nanocomposites.

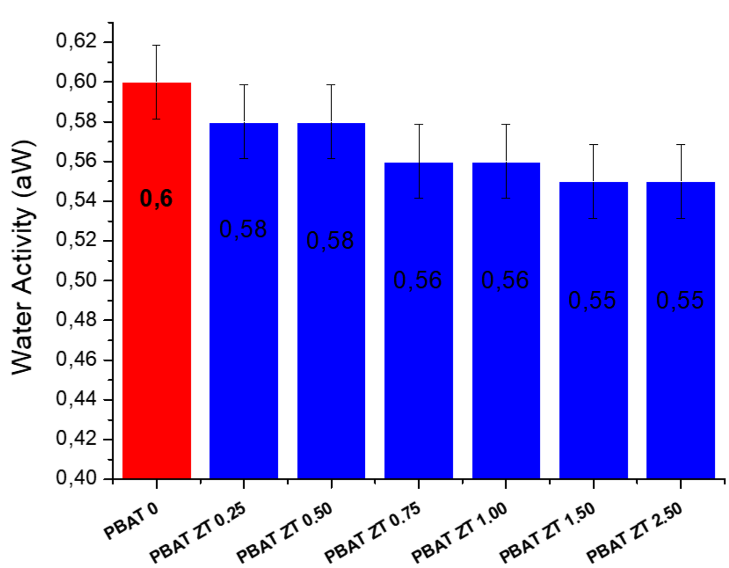

Figure 8. Water activity (aw) measurements of pure PBAT and its nanocomposites.

Overall, the results highlight the potential of PBAT/ZnO/TiO_2 films for the development of high-performance food packaging systems capable of effectively controlling water activity, limiting microbial proliferation, and reducing moisture-induced degradation processes.

Acknowledgments

The authors would like to thank the Instituto de Macromoléculas Professora Eloisa Mano of the Federal University of Rio de Janeiro (UFRJ) for the infrastructure and support provided for the development of this work

REFERENCES

AHMAD AA, ALSAAD AM, ALJARRAH IA, AL BATAINEH QM & TELFAH AD. 2022. Optical, electronic, and structural properties of different nanostructured ZnO morphologies. Eur Phys J Plus 137: 752.

AL-AMIN M, DEY SC, RASHID TU, ASHADUZZAMAN M & SHAMSUDDIN SM. 2016. Solar Assisted Photocatalytic Degradation of Reactive Azo Dyes in Presence of Anatase Titanium Dioxide. Int J Latest Res Eng Technol 2: 14-21.

ARSSANASUWAN N, THREEPOPNATKUL P & SITTATTRAKUL A. 2020. Effect of titanium dioxide on the properties of poly(butylene adipate-co-terephthalate) films. IOP Conf Ser: Mater Sci Eng 965: 012016.

BATOOL M, ABID M, KHURSHID S, BASHIR T, ISMAIL M, RAZAQ M & JAMIL M. 2022. Quality control of nano-food packing material for grapes (Vitis vinifera) based on ZnO and polylactic acid (PLA) biofilm. Arab J Sci Eng 47: 319-331.

BEUCHAT LR. 1982. Microbial stability as affected by water activity. Cereal Foods World 26(7): 345-349.

BHEEMANENI G, SARAVANA S & KANDASWAMY R. 2018. Processing and characterization of poly(butylene adipate-co-terephthalate)/wollastonite biocomposites for medical applications. Mater Today Proc 5(1): 1807-1816.

CAPELEZZO AP, MOHR LC, DALCANTON F, BARRETA CRDM, MARTINS MAPM, FIORI MA & MELLO JMMD. 2018. Polímero biodegradável antimicrobiano através da aditivação com compostos à base de zinco. Quím Nova 41(4): https://doi.org/10.21577/0100-4042.20170187.

CARDOSO ECL, PARRA DF, SCAGLIUSI SR, SALES RM, CAVIQUIOLI F & LUGAO AB. 2019. Study of Bio-Based Foams Prepared from PBAT/PLA Reinforced with Bio-Calcium Carbonate and Compatibilized with Gamma Radiation. In: Almayah BA (Ed), Use of Gamma Radiation Techniques in Peaceful Applications. IntechOpen, London, p. 139-156.

CASTRO DPD, GARCIA RHL & SILVA LGDAE. 2020. Characterization using x-ray diffraction and study of the crystallinity of the thermoplastic starch/poly(butylene adipate-co-terephthalate) blends irradiated by gamma rays. Braz J Dev 6(3): 9635-9643.

CHAROENSRI K, RODWIHOK C, KO SH, WONGRATANAPHISAN D & PARK HJ. 2021. Enhanced antimicrobial and physical properties of poly(butylene adipate-co-terephthalate)/zinc oxide/reduced graphene oxide ternary nanocomposite films. Mater Today Commun 28: 102586.

CHEN P, XIE F, TANG F & MCNALLY T. 2020. Structure and properties of thermomechanically processed chitosan/carboxymethyl cellulose/graphene oxide polyelectrolyte complexed bionanocomposites. Int J Biol Macromol 158: 420-429.

CHOUGALA L, YATNATTI M, LINGANAGOUDAR R, KAMBLE R & KADADEVARMATH J. 2017. A Simple Approach on Synthesis of TiO_2 Nanoparticles and its Application in dye Sensitized Solar Cells. J Nano- Electron Phys 9(4): 04005-1-04005-6.

CUNHA TA, VERMEULEN-SERPA KM, GRILO EC, LEITE-LAIS L, BRANDÃO-NETO J & VALE SHL. 2022. Association between zinc and body composition: An integrative review. J Trace Elem Med Biol 71: 126940.

DA ROCHA LVM, DA SILVA PSRC & TAVARES MIB. 2023. Comparative Study Of Poly(Butylene Adipate Co-Terephthalate) Nanocomposites With Zinc And Molybdenum Oxides. Seven Editora, p. 218-224.

DA SILVA CG, KANO FS & ROSA DS. 2020. Lignocellulosic Nanofiber from Eucalyptus Waste by a Green Process and Their Influence in Bionanocomposites. Waste Biomass Valor 11: 3761-3774.

DE PERES ML, DELUCIS RDE A, AMICO SC & GATTO DA. 2019. Zinc oxide nanoparticles from microwave-assisted solvothermal process: Photocatalytic performance and use for wood protection against xylophagous fungus. Nanomater Nanotechnol 9. DOI:10.1177/1847980419876201.

DE SOUZA AG, KOMATSU L, BARBOSA R, PARRA D & ROSA D. 2022. The effect of ZnO nanoparticles as ag-carrier in PBAT for antimicrobial films. Polym Bull 79: 4031-4048.

HAIDER AJ, AL-ANBARI RH, KADHIM GR & SALAME CT. 2017. Exploring potential Environmental applications of TiO_2 Nanoparticles. Energy Procedia 119: 332-345.

HANDORE K, BHAVSAR S, HORNE A, CHHATTISE P, MOHITE K, AMBEKAR J, PANDE N & CHABUKSWAR V. 2014. Novel Green Route of Synthesis of ZnO Nanoparticles by Using Natural Biodegradable Polymer and Its Application as a Catalyst for Oxidation of Aldehydes. J Macromol Sci A 51(12): 941-947.

HONG R, PAN T, QIAN J & LI H. 2006. Synthesis and surface modification of ZnO nanoparticles. Chem Eng J 119(2-3): 71-81.

HOU X, XUE Z, LIU J, YAN M, XIA Y & MA Z. 2019. Characterization and property investigation of novel eco-friendly agar/carrageenan/TiO_2 nanocomposite films. J Appl Polym Sci 136: 47113.

IULIANELLI GCV, COSTA LV, SILVA PSC & SANTOS FA. 2023. Evaluation of Fully Biodegradable PLA/PHB Blend Filled with Microcrystalline Celluloses. Mat Res 26: https://doi.org/10.1590/1980-5373-MR-2022-0433.

JANAKI AC, SAILATHA E & GUNASEKARAN S. 2015. Synthesis, characteristics and antimicrobial activity of ZnO nanoparticles. Spectrochim Acta A 144: 17-22.

JAYBHAYE S, SHINDE N, JAYBHAYE S & NARAYAN H. 2022. Photocatalytic Degradation of Organic Dyes Using Titanium Dioxide (TiO_2) and Mg-TiO_2 Nanoparticles. J Nanotechnol Nanomater 3(2): 67-76.

JIAN J, XIANGBIN X & XIANBO H. 2020. An overview on synthesis, properties and applications of poly(butylene-adipate-co-terephthalate)-PBAT. Adv Ind Eng Polym Res 3(1): 19-26.

KODITHUWAKKU P, JAYASUNDARA D, MUNAWEERA I, JAYASINGHE R, THORADENIYA T, WEERASEKERA M & KOTTEGODA N. 2022. A review on recent developments in structural modification of TiO_2 for food packaging applications. Prog Solid State Chem 67: 1-24.

LA FUENTE CIA, MANIGLIA BC & TADINI CC. 2023. Biodegradable polymers: A review about biodegradation and its implications and applications. Packag Technol Sci 36(2): 81-95.

LE V-G ET AL. 2024. Microplastics in aquaculture environments: Current occurrence, adverse effects, ecological risk, and nature-based mitigation solutions. Mar Pollut Bull 209: 117168.

MASUD RA, ISLAM MDS, HAQUE P, KHAN MNI, SHAHRUZZAMAN M, KHAN M, TAKAFUJI M & RAHMAN MM. 2020. Preparation of novel chitosan/poly(ethylene glycol)/ZnO bionanocomposite for wound healing application. Materialia 12: 100785.

MAYRINCK C, RAPHAEL E, FERRARI JF & SCHIAVON MA. 2014. Synthesis, Properties and Applications of Nanostructured Zinc Oxide. Rev Virtual Quím 6: 1185-1204.

MENDES JF, MARTINS JT, MANRICH A, NETO SAR, PINHEIRO ACM, MATTOSO LHC & MARTINS MA. 2019. Development and physical-chemical properties of pectin film reinforced with spent coffee grounds by continuous casting. Carbohydr Polym 210: 92-99.

MESGARI M, AALAMI AH & SAHEBKAR A. 2021. Antimicrobial activities of chitosan/titanium dioxide composites as a biological nanolayer for food preservation. Int J Biol Macromol 176: 530-539.

MUROI F, TACHIBANA Y, SOULENTHONE P, YAMAMOTO K, MIZUNO T, SAKURAI T, KOBAYASHI Y & KASUYA K. 2017. Characterization of a poly(butylene adipate-co-terephthalate) hydrolase from the aerobic mesophilic bacterium Bacillus pumilus. Polym Degrad Stab 137: 11-22.

PASCARIU P, HOMOCIANU M, OLARU N, AIRINEI A & IONESCU O. 2020. New Electrospun ZnO:MoO_3 Nanostructures: Preparation, Characterization and Photocatalytic Performance. Nanomaterials 10(8): 1476.

PAVANI NM, MACENA DA, TAMASHIRO JR, SILVA LHPD, ALMEIDA MPBD & KINOSHITA AMO. 2023. Nanopartículas De Dióxido De Titânio E Óxido De Zinco: Síntese, Caracterização E Ação Fotocatalítica Em Efluentes Industriais. Colloq Exactarum 14(1): 185-192.

PENS CJS, KLUG TV, STOLL L, IZIDORO F, FLORES SH & RIOS AO. 2024. Poly (lactic acid) and its improved properties by some modifications for food packaging applications: A review. Food Packaging and Shelf Life 41: https://doi.org/10.1016/j.fpsl.2023.101230.

PRAVEEN P, VIRUTHAGIRI G, MUGUNDAN S & SHANMUGAM N. 2014. Structural, optical and morphological analyses of pristine titanium di-oxide nanoparticles-Synthesized via sol-gel route. Spectrochim Acta A 117: 622-629.

QUADRI TW, OLASUNKANMI LO, FAYEMI OE, SOLOMON MM & EBENSO EE. 2017. Zinc Oxide Nanocomposites of Selected Polymers: Synthesis, Characterization, and Corrosion Inhibition Studies on Mild Steel in HCl Solution. ACS Omega 2(11): 8421-8437.

RAJAKUMAR G, RAHUMAN AA, ROOPA NSM, KHANNA VG, ELANGO G, KAMARAJ C, ZAHIR AA & VELAYUTHAM K. 2012. Fungus-mediated biosynthesis and characterization of TiO_2 nanoparticles and their activity against pathogenic bacteria. Spectrochim Acta A 91: 23-29.

RAMESHKUMAR S, SHAIJU P, O'CONNOR KE & BABU PR. 2020. Bio-based and biodegradable polymers - State-of-the-art, challenges and emerging trends. Curr Opin Green Sustain Chem 21: 75-81.

RIZKY SALSABILA A, BAYU A & NANDIYANTO D. 2023. Biodegradable Food Packaging with The Addition of ZnO Nanoparticles: A Bibliometric Analysis with Computational Mapping using VOSviewer. Fullerene J Chem 7(2): 111-119.

SABARISH R, JASILA K, ASWATHY J, JYOTISHKUMAR P & SUCHART S. 2024. Mechanical and morphological properties of nanocomposite films for food packaging applications. Biocomposites for Industrial Applications, 387-404. https://doi.org/10.1016/B978-0-323-91866-4.00012-3.

SANG L, ZHAO Y & BURDA C. 2014. TiO_2 nanoparticles as functional building blocks. Chem Rev 114(19): 9283-9318.

SMAOUI S, CHÉRIF I, HLIMA BH, KHAN MU, REBEZOV M, THIRUVENGADAM M, SARKAR T, SHARIATI MA & LORENZO JM. 2023. Zinc oxide nanoparticles in meat packaging: A systematic review of recent literature. Food Packag Shelf Life 36: 101045.

SUWARNKAR MB ET AL. 2014. Enhanced photocatalytic activity of Ag doped TiO_2 nanoparticles synthesized by a microwave assisted method. Ceram Int 40(4): 5489-5496.

TAVARES LB, ITO NM, SALVADORI MC, DOS SANTOS DJ & ROSA DS. 2018. PBAT/kraft lignin blend in flexible laminated food packaging: Peeling resistance and thermal degradability. Polym Test 67: 169-176.

THABIT HA & KABIR NA. 2018. The study of X-ray effect on structural, morphology and optical properties of ZnO nanopowder. Nucl Instrum Methods Phys Res B 436: 278-284.

THIYAGU TT, GOKILAKRISHNAN G, UVARAJA VC, MARIDURAI T & PRAKASH VA. 2022. Effect of SiO_2/TiO_2 and ZnO nanoparticle on cardanol oil compatibilized PLA/PBAT biocomposite packaging film. Silicon 14: 3795-3808.

VALENTIM ACS, TAVARES MIB & SILVA EO. 2014. Efeito da adição de TiO_2 nas propriedades térmicas e na cristalinidade do copolímero de etileno/acetato de vinila. Quím Nova 37: 255-259.

VALERIO TL, MAIA GAR, GONÇALVES LF, VIOMAR A, BANCZEK EDP & RODRIGUES PRP. 2019. Study of the Nb_2O_5 insertion in ZnO to dye-sensitized solar cells. Mater Res 22: e20180864.

VENKATESAN R & RAJESWARI N. 2017a. ZnO/PBAT nanocomposite films: Investigation on the mechanical and biological activity for food packaging. Polym Adv Technol 28(1): 20-27.

VENKATESAN R & RAJESWARI N. 2017b. TiO_2 nanoparticles/poly(butylene adipate-co-terephthalate) bionanocomposite films for packaging applications. Polym Adv Technol 28(12): 1699-1706.

WANG Y, HE Y, LAI Q & FAN M. 2014. Review of the progress in preparing nano TiO_2: An important environmental engineering material. J Environ Sci 26(11): 2139-2177.

YADAV B, GUPTA P & KUMAR V ET AL. 2024. Potential health, environmental implication of microplastics: A review on its detection. J Contam Hydrol 268: 104467.

YANG Y, DOUDRICK K, BI X, HRISTOVSKI K, HERCULES P, WESTERHOFF P & KAEGI R. 2014. Characterization of food-grade titanium dioxide: the presence of nanosized particles. Environ Sci Technol 48(11): 6391-6400.

YIN B, FANG L, HU J, TANG AQ, WEI WH & HE J. 2010. Preparation and properties of super-hydrophobic coating on magnesium alloy. Appl Surf Sci 257(5): 1666-1671.

ZEHETMEYER G, MEIRA SMM, SCHEIBEL JM, DE OLIVEIRA RVB, BRANDELLI A & SOARES RMD. 2016. Influence of melt processing on biodegradable nisin-PBAT films intended for active food packaging applications. J Appl Polym Sci 133(13): 43212.

ZHANG W & RHIM JW. 2022. Titanium dioxide (TiO_2) for the manufacture of multifunctional active food packaging films. Food Packag Shelf Life 31: 100806.

How to cite

FERREIRA CSG, SOUZA PS, LACERDA DS, RODRIGUES FAM & IULIANELLI GCV. 2025. Biodegradable nanocomposite films containing combined ZnO and TiO_2 nanoparticles in PBAT: A strategy to mitigate microplastic persistence from food packaging. An Acad Bras Cienc 97: e20250559. DOI 10.1590/0001-3765202520250559.

Manuscript received on May 20, 2025;
accepted for publication on September 3, 2025

CAMILA S.G. FERREIRA[1]
https://orcid.org/0000-0002-2466-136X

PRISCILA S. E SOUZA[1]
https://orcid.org/0009-0004-0358-909X

DILMA S. LACERDA[1]
https://orcid.org/0009-0009-9743-3040

FERNANDO A.M. RODRIGUES[2]
https://orcid.org/0000-0002-3175-1160

GISELE CRISTINA V. IULIANELLI[1]
https://orcid.org/0000-0003-2511-4875

[1]Universidade Federal do Rio de Janeiro, Instituto de Macromoléculas Professora Eloisa Mano. Av. Horácio Macedo, 2030, Centro de Tecnologia – Bloco J, Cidade Universitária, 21941-598 Rio de Janeiro, RJ, Brazil

[2]Universidade do Estado do Rio de Janeiro (UERJ), Instituto de Química. Rua São Francisco Xavier, 524, Maracanã, 20950-000 Rio de Janeiro, RJ, Brazil

Correspondence to: **Camila Spinola Gonçalves Ferreira**
E-mail spinola.camila@gmail.com

Author contributions

Camila Spinola Gonçalves Ferreira: Formal analysis (Lead), Investigation (lead), methodology (equal), writing-original draft (lead), writing-review & editing (equal). Priscila da Silva e Souza: Methodology (equal), writing original draft (supporting). Dilma dos Santos Lacerda: Formal analysis (supporting), Methodology (supporting), writing original draft (supporting). Fernando Altino Medeiros Rodrigues: Formal analysis (supporting), Methodology (supporting), writing original draft (supporting). Gisele Cristina Valle Iulianelli: conceptualization (Lead), Methodology (equal), Project administration (Lead), supervision (Lead), writing original draft (supporting), writing review and editing (equal). All authors have read and agreed to the published version of the manuscript.